Electronic Supplementary Material (ESI) for Chemical Communications.

Electronic Supplementary Information (ESI) for:

Design and Synthesis of Capped-Paddlewheel-Based Porous Coordination Cages

Gregory R. Lorzing,[a,b] Aeri J. Gosselin,[a] Brian S. Lindner,[a] Rameswar Bhattacharjee,[c] Glenn P. A. Yap,[a] Stavros Caratzoulas,[c] and Eric D. Bloch*[a,b,c]

*edb@udel.edu

[a]Department of Chemistry and Biochemistry, University of Delaware, Newark, Delaware, 19716, USA

[b]Center for Neutron Science, Department of Chemical and Biomolecular Engineering, University of Delaware, Newark, Delaware, 19716, USA

[c]Catalysis Center for Energy Innovation (CCEI), University of Delaware, Newark, Delaware, 19716, USA

List of Contents

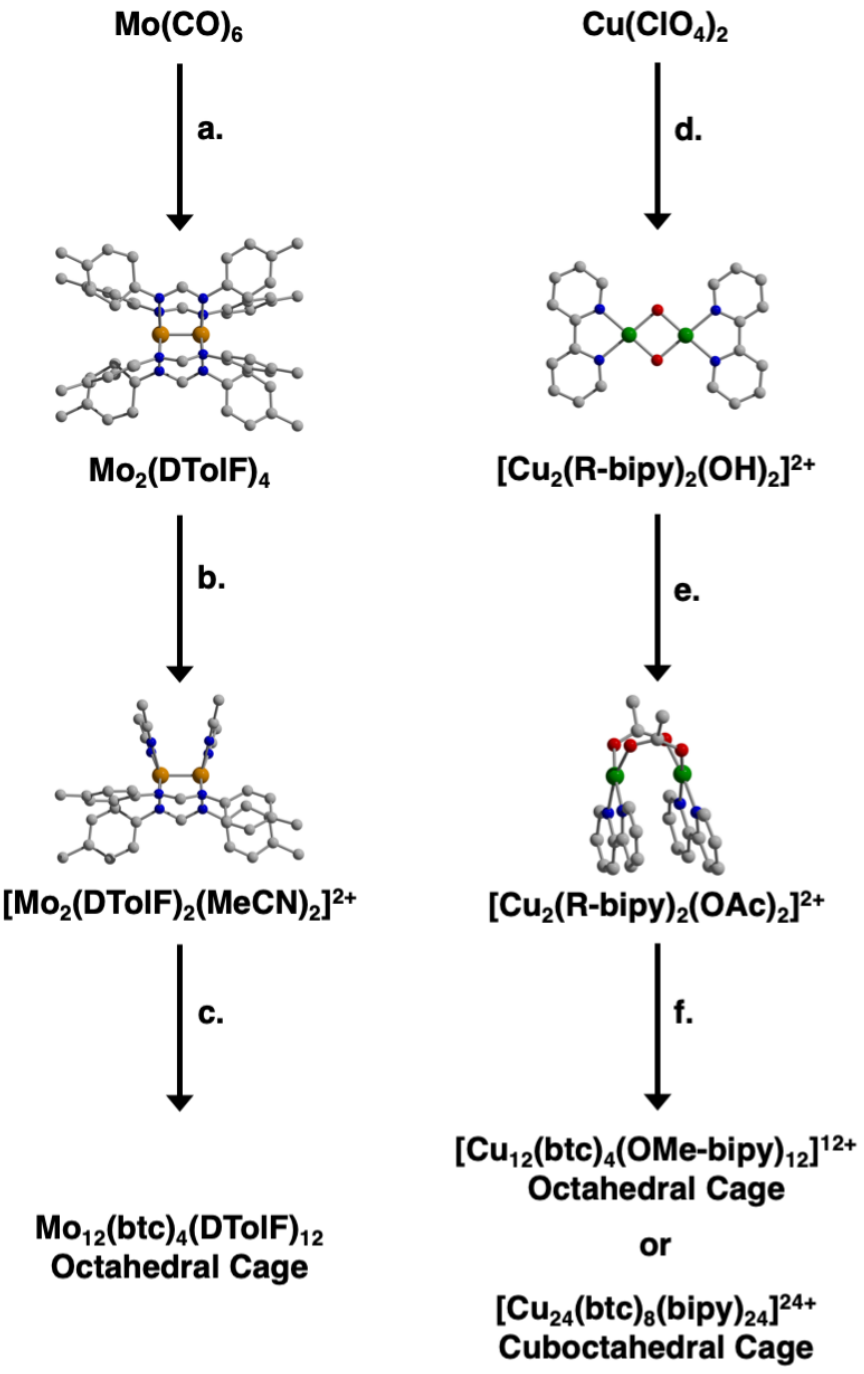

Scheme 1. Capping strategy to afford discrete, porous cages. Here formamidinate ligands cap cis-divacant sites on molybdenum(II) paddlewheel units whereas functionalized bipyridine ligands are necessary for copper(II) paddlewheels. Synthetic conditions: a. HDTolF in *o*-dichlorobenzene; b. trimethyloxonium tetrafluoroborate in MeCN; c. tetrabutylammonium 1,3,5-benzenetricarboxylate in MeCN; d. 2,2-bipyridine in aqueous NaOH; e. aqueous acetic acid; f. 1,3,5-benzenetricarboxylic acid in methanol**.**

Experimental Section

General Considerations. All Reagents were obtained from commercial venders and used without further purification, excluding solvents used for air sensitive procedures. Air sensitive products used solvent obtained from a solvent purification system and then stored in a glove box over 4 Å sieves. Thermogravimetric analyses (TGA) were carried out from 50 °C to 600 °C at a 2 °C min^{-1} heating rate with a TA Q5000 SA under a nitrogen environment. All adsorption measurements were obtained on a Micromeritics 3Flex.

Caution: Perchlorate salts are known to be explosive especially when anhydrous.

Synthesis of HDTolF. To a 100mL round bottom flask, p-tolyl-aniline (21.43 g, 200 mmol) and triethyl orthoformate (16.13 mL, 100 mmol) were added. The reaction was heated to 140 °C until no more ethanol distilled off. Upon cooling, the product was recrystallized in hot toluene to yield a white crystalline powder (19.8 g, 88.3%). ^1H NMR (400 MHz, 25 °C, $CDCl_3$) 8.14 (s, 1H), 7.12 (d, J = 8 Hz, 4H), 6.95 (d, J= 8 Hz, 4H), 2.32 (s, 6H).

Synthesis of $Mo_2(DTolF)_4$.[1] $Mo(CO)_6$ (2 g, 7.57 mmol) and HDTolF (5.097 g, 22.726 mmol) were added to a mixture of ortho-dichloromethane and hexane in a 2:1 ratio under N_2. The reaction was heated to reflux at 160 °C for 24 h. Upon cooling, the reaction was brought into a glove box, filtered and washed with minimal diethyl ether to yield a yellow crystalline product. ^1H NMR (400 MHz, 25 °C, DMF-d7) 8.58 (s, 1H), 6.78 (d, J = 8 Hz, 4H), 6.24 (d, J = 8 Hz, 4H), 2.21 (s, 6H).

Synthesis of *cis*-$[Mo_2(DTolF)_2(MeCN)_4][BF_4]_2$.[2] $Mo_2(DTolF)_4$ (800 mg, 0.679 mmol), trimethyloxonium tetrafluoroborate (602 mg, 4.07 mmol) and acetonitrile (250 mL) were added to a 500 mL Schlenk flask. The Schlenk flask was brought out of the box and 5 drops of deoxygenated water were added to the reaction mixture. Overnight, the reaction turned from a cloudy yellow to a bright, clear red solution. The solvent was removed under vacuum, brought into the glove box and washed with 100 mL of diethyl ether. The resulting solid was then dissolved in a 19:1 dichloromethane/acetonitrile mixture and layered with diethyl ether. Upon mixing, the product precipitated out of solution as a red crystalline solid. The powder was collected via vacuum filtration and stored in the glove box. The product yield was essentially quantitative. ^1H NMR (400 MHz, 25 °C, THF-d8) 7.38 (d, J = 8.4 Hz, 8H), 7.28 (d, J = 8.4 Hz, 8H), 2.35 (s, 12H), 1.95 (s, 12H).

Synthesis of $Mo_{12}(btc)_4(DTolF)_{12}$.[3] In the glove box, *cis*-$[Mo_2(DTolF)_2(MeCN)_4][BF_4]_2$ (0.1 g, 0.102 mmol) was dissolved in acetonitrile (5 mL) in a 20 mL scintillation vial. $[TBA]_3[btc]$ (0.063 g, 0.068 mmol) was dissolved in acetonitrile (5 mL) in a 20 mL scintillation vial. The $[TBA]_3[btc]$ solution was then added into the Mo solution via pipet. Solid precipitate immediately crashed out of solution. The powder was collected via vacuum filtration and washed with acetonitrile until the filtrate was colorless. The orange powder was dissolved in dichloromethane and layered with acetonitrile to yield large red crystals. ^1H NMR (400 MHz, 25 ºC, $CDCl_3$) 9.38 (s, 12H), 8.57 (s, 12H), 6.80 (d, J = 8 Hz, 48H), 6.51 (d, J = 8 Hz, 48H), 2.2 (s, 72H).

Synthesis of $[Cu_2(bipy)_2(\mu\text{-}OH)_2][ClO_4]_2$.[4] This procedure was done analogous to a previous report. Generally, $Cu(ClO_4)_2 \cdot 6\ H_2O$ (1 g, 2.7 mmol) was dissolved in DI H_2O (60 mL) in a 400 mL beaker. The pH of the solution was tuned to 9.25 by dropwise addition of 1M NaOH solution while stirring. 2,2'-bipyridine (0.422 g, 2.7 mmol) was dissolved in methanol (5 mL) and then added to the copper solution. The solution was left to stir at room temperature for 1 hour until lavender solid precipitated out. The solid was collected via vacuum filtration. Solid was then washed with diethyl ether (30mL x3) resulting in dry lavender solid (0.76 g, 78.5 %).

Synthesis of $[Cu_2(bipy)_2(OAc)_2][ClO_4]_2$.[5] This compound was made as previously reported.

Synthesis of $[Cu_{24}(btc)_8(bipy)_{24}][ClO_4]_{24}$. $[Cu_2(bipy)_2(OAc)_2][ClO_4]_2$ (0.423 g, 0.558 mmol) was dissolved in methanol (60 mL) in a 100 mL RBF. Trimesic acid (0.078 g, 0.372 mmol) was dissolved in methanol (20 mL) in a 20 mL scintillation vial. The trimesic acid solution was added to a 60 mL addition funnel and added dropwise over ten minutes to the copper solution while stirring. The solution immediately became cloudy upon addition. The solution was allowed to stir at room temperature for three hours. The resulting solid was collected via vacuum filtration and was with methanol (30 mL x3). Crude product was collected as light blue powder (0.252 g). The solid was re-crystallized by reverse diffusion of a saturated acetonitrile solution (10 mL in a 20 mL scintillation vial) solution into methanol in a 100 mL VWR jar.

Synthesis of $[Cu_2(\mu\text{-}OH)_2(OMe\text{-}bipy)_2][ClO_4]_2$. This compound was made analougous to that of the $[Cu_2(bipy)_2(\mu\text{-}OH)_2][ClO_4]_2$ compound. Generally, Generally, $Cu(ClO_4)_2 \cdot 6\ H_2O$ (1 g, 2.7 mmol) was dissolved in DI H_2O and methanol (50 mL/50 mL) in a 400 mL beaker. The pH of the solution was tuned to 9.25 by dropwise addition of 1M NaOH solution while stirring. 4,4'-dimethoxy-2,2'-bipyridine (0.582 g, 2.7 mmol) was dissolved in methanol (100 mL) and then added to the copper solution. The solution was left to stir at room temperature for 1 hour until light blue solid precipitated out. The solid was collected via vacuum filtration. Solid was then washed with diethyl ether (30mL x3) resulting in dry blue solid (0.98 g, 90 %).

Synthesis of $[Cu_2(OAc)_2(OMe\text{-}bipy)_2][ClO_4]_2$. This compound was made analogous to that of Synthesis of $[Cu_2(bipy)_2(OAc)_2][ClO_4]_2$.

Synthesis of $[Cu_{12}(btc)_4(OMe\text{-}bipy)_{12}][ClO_4]_{12}$. $[Cu_2(OAc)_2(OMe\text{-}bipy)_2][ClO_4]_2$ (0.490 g, 0.56 mmol) was dissolved in methanol (100 mL) in a 250 mL RBF. Trimesic acid (0.049 g, 0.234 mmol) was dissolved in methanol (20 mL) in a 20 mL scintillation vial. The trimesic acid solution was added to a 60 mL addition funnel and added dropwise over ten minutes to the copper solution while stirring. The solution immediately became cloudy upon addition. The solution was allowed to stir at room temperature for three hours. The resulting solid was collected via vacuum filtration and was with methanol (30 mL x3). Crude product was collected as light blue powder (0.199 g). The solid was re-crystallized by diffusion of diethyl ether into a saturated acetonitrile solution (10 mL in a 20 mL scintillation vial) in a 100 mL VWR jar in a 5 °C refrigerator.

X-Ray Crystallography

X-ray structural analysis for $Mo_{12}(btc)_4(DtolF)_{12}$, $Mo_2(DTolF)_2(MeCN)_2(BF_4)_2$, $[Cu_{24}(btc)_8(bipy)_{24}][ClO_4]_{24}$, and $[Cu_{12}(btc)_4(OMe\text{-}bipy)_{12}][ClO_4]_{12}$: Crystals were mounted using viscous oil onto a plastic mesh and cooled to the data collection temperature. Data were collected on a Bruker-AXS APEX II DUO CCD diffractometer with Cu-Kα radiation (λ = 1.54178 Å) focused with Goebel mirrors for $Mo_{12}(btc)_4(DtolF)_{12}$, $[Cu_{24}(btc)_8(bipy)_{24}][ClO_4]_{24}$, and $[Cu_{12}(btc)_4(OMe\text{-}bipy)_{12}][ClO_4]_{12}$; and, with graphite monochromated Mo-Kα radiation (λ=0.71073 Å) for $Mo_2(DTolF)_2(MeCN)_2(BF_4)_2$. Unit cell parameters were obtained from 36 data frames, 0.5° ω, from three different sections of the Ewald sphere. The unit-cell dimensions, equivalent reflections and systematic absences in the diffraction data are consistent with *Cc*, and *C*2/*c*. for $Mo_{12}(btc)_4(DtolF)_{12}$; and with *P*4*nc* and *P*4/*mnc*. No symmetry higher than triclinic was observed for $Mo_2(DTolF)_2(MeCN)_2(BF_4)_2$ and $[Cu_{12}(btc)_4(OMe\text{-}bipy)_{12}][ClO_4]_{12}$. Refinement in the centrosymmetric space group options yielded chemically reasonable and computationally stable results of refinement. The data were treated with multi-scan absorption corrections.[6] Structures were solved using intrinsic phasing methods[7] and refined with full-matrix, least-squares procedures on F^2.[8] The compound molecule is located at a two-fold axis in $Mo_{12}(btc)_4(DtolF)_{12}$, and, at a four-fold axis and mirror plane in $[Cu_{24}(btc)_8(bipy)_{24}][ClO_4]_{24}$. Two symmetry-unique but chemically identical compound molecules with one molecule of cocrystallized acetonitrile solvent were located in the asymmetric unit of $Mo_2(DTolF)_2(MeCN)_2(BF_4)_2$ and $[Cu_{12}(btc)_4(OMe\text{-}bipy)_{12}][ClO_4]_{12}$.

The disordered cell contents of highly porous metal-organic framework (MOF) and metal-organic polyhedra (MOP) complexes result in diffraction data that are limited in coverage and resolution. As a result, it is common to have multiple restraints and constraints, incompletely identified moieties, and high residuals in the structural model.[9] In the case of $[Cu_{12}(btc)_4(OMe\text{-}bipy)_{12}][ClO_4]_{12}$, the data crystal was multiple resulting in even poorer quality data that required modelling the organic moieties as rigid groups but the data reported herein represented the best of several trials and clearly shows this species to form Cu12 MOPs instead of Cu24.The formulas reported herein reflect only the atoms that were discretely modeled. Presumably disordered solvent molecules (and counterions in the case of $[Cu_{24}(btc)_8(bipy)_{24}][ClO_4]_{24}$) were treated as diffused contributions using Squeeze.[10] Phenyl groups were constrained to have idealized hexagonal geometry in $Mo_2(DTolF)_2(MeCN)_2(BF_4)_2$. Two phenyl groups in $Mo_2(DTolF)_2(MeCN)_2(BF_4)_2$ were located disordered in two positions with refined site occupancies of 51/49 and 66/34. Chemically equivalent atoms in the disordered contributions were constrained with equal atomic displacement parameters. Global three-dimensional rigid bond restraints on anisotropic displacement parameters were applied. Non-hydrogen atoms were refined with anisotropic displacement parameters. Hydrogen atoms were treated as idealized contributions with geometrically calculated positions and with U_{iso} equal to 1.2 U_{eq} (1.5 U_{eq} for methyl) of the attached atom. Atomic scattering factors are contained in the SHELXTL program library.[8] The structures have been deposited at the Cambridge Structural Database under the following CCDC depositary numbers: 1839943, 1839944, 1846389 and 1940761.

Computational Methods

All calculations were performed at the M06-L/6-31G(d,p)//M06-L/6-311G(3df,2pd) theory level, namely, structure optimizations at the M06-L/6-31G(d,p) level were followed by single-point calculations using the triple-ζ basis set. We selected the M06-L functional as it is well balanced for first-row transition metal complexes.[11,12] Frequency analysis of the M06-L/6-31G(d,p) potential energy surface confirmed the absence of imaginary frequencies at the located stationary points. All calculations were performed in Gaussian 09.[13]

We investigated the stability of restricted singlet, unrestricted ferromagnetic triplet, and unrestricted broken-symmetry anti-ferromagnetic singlet wave functions; the anti-ferromagnetic wave function was set up using the molecular orbitals from the optimized ferromagnetic wave function. All three wave functions proved to be stable, with the broken-symmetry one being the lowest in energy. The restricted singlet is about 15 kcal/mol higher in energy than the ferromagnetic triplet while the latter, high-spin state, lies less than 1 kcal/mol higher than the anti-ferromagnetic state, suggesting a statistical mix of the anti-ferromagnetic and ferromagnetic states at finite temperature. The expectation value of the square of the spin operator over the broken symmetry state, $\langle S^2 \rangle_{BS}$, is 0.9869 a.u., for the copper complex with the unsubstituted bipyridine ligand and 0.9915 a.u., for the complex with the methoxylated bipyridine ligand.

Magnetic coupling constants (*J*) were estimated using the Yamaguchi formula:[14,15,16]

$$J = -\frac{E_{HS} - E_{BS}}{\langle S^2 \rangle_{HS} - \langle S^2 \rangle_{BS}},$$

where HS and BS stand for high-spin and broken-symmetry, respectively. $\langle S^2 \rangle_{HS} = 2.000$ after annihilation of spin contaminants, in all cases.

For both gas-phase optimized complexes, the ground state is the broken symmetry, anti-ferromagnetically coupled singlet. It is, however, only about 0.5 kcal/mol more stable than the ferromagnetic triplet. The complexes are in a statistical mix of the two states. Exchange coupling constants for L=bipy and OMe-bipy are as follows J=-129 cm^{-1} and J=-120 cm^{-1} . The two Cu atoms are slightly closer to each other in the unsubstituted complex. Overall, the geometries of the two complexes don't differ in any significant way. The methoxy group doesn't seem to have any effect on the coordination of the acetate. The lengths of all the coordination bonds are compiled in a table below.

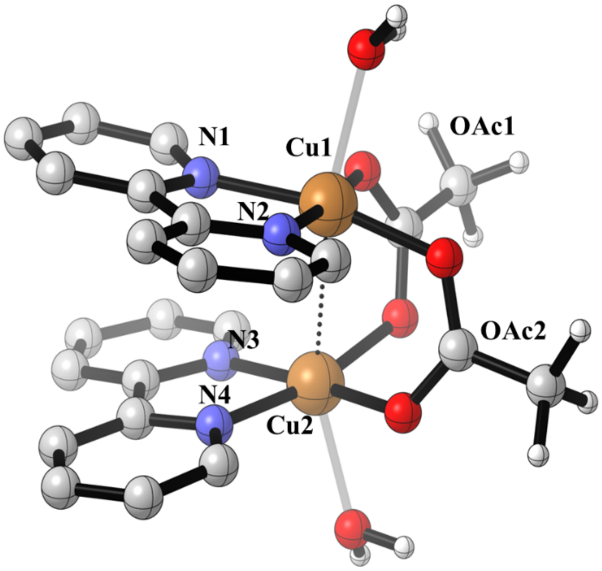

Cu1-Cu2 = 2.85
Cu1-N1 &Cu1-N2 = 2.0
Cu1-OH2 = 2.22
Cu1-OAc1 &Cu1-OAc2 = 1.95
Cu2-N3 &Cu1-N4 = 2.0
Cu1-OH2 = 2.22
Cu2-OAc1 &Cu2-OAc2 = 1.95
bpy-bpy ~ 3.5

Figure S1. Geometry optimization of in $[Cu_{24}(btc)_8(bipy)_{24}][ClO_4]_{24}$

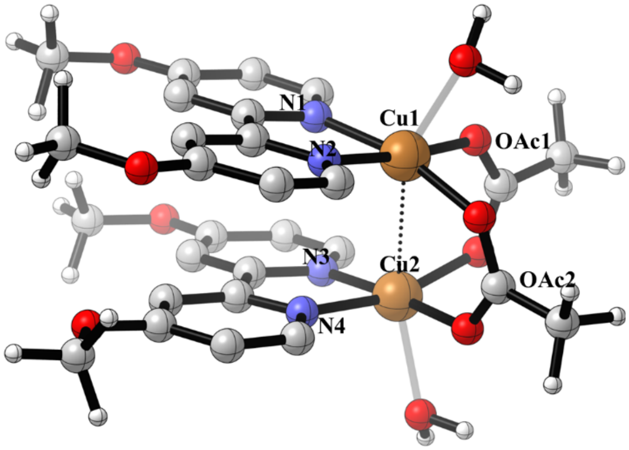

Cu1-Cu2 = 2.88
Cu1-N1 = 1.98
Cu1-N2 = 1.99
Cu1-OH = 2.23
Cu1-OAc1 = 1.94
Cu1-OAc2 = 1.95
Cu2-N3 = 1.99
Cu1-N4 = 1.99
Cu2-OH =2.22
Cu2-OAc1 = 1.93
Cu2-OAc2 = 1.96
bpy-bpy ~ 3.2

Figure S2. Geometry optimization of $[Cu_{12}(btc)_4(OMe\text{-}bipy)_{12}][ClO_4]_{12}$

	bpy	**bpy-OMe**
Atom-Atom	$d_{\text{atom-atom}}$ (Å)	$d_{\text{atom-atom}}$ (Å)
Cu1-Cu2	2.85	2.88
Cu1-N1	2.00	1.98
Cu1-N2	2.00	1.99
Cu1-OH$_2$	2.22	2.23
Cu1-O^{1}Ac1	1.95	1.94
Cu1-O^{1}Ac2	1.95	1.95
Cu2-N3	2.00	1.99
Cu1-N4	2.00	1.99
Cu1-OH$_2$	2.22	2.22
Cu2-O^{2}Ac1	1.95	1.93
Cu2-O^{2}Ac2	1.95	1.96
bpy-bpy ~ 3.5	3.50	3.20

Table S1. Table of bond distances in the two geometry optimized copper cages.

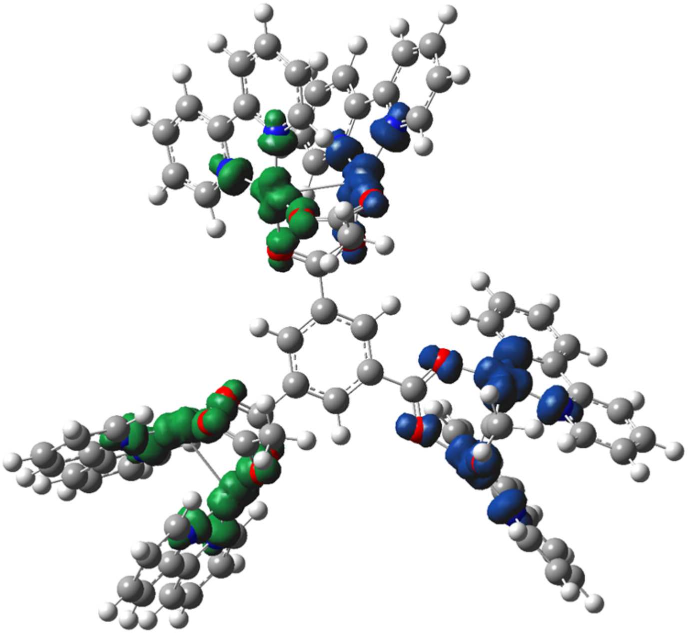

Figure S3. Spin density of in $[Cu_{24}(btc)_8(bipy)_{24}][ClO_4]_{24}$

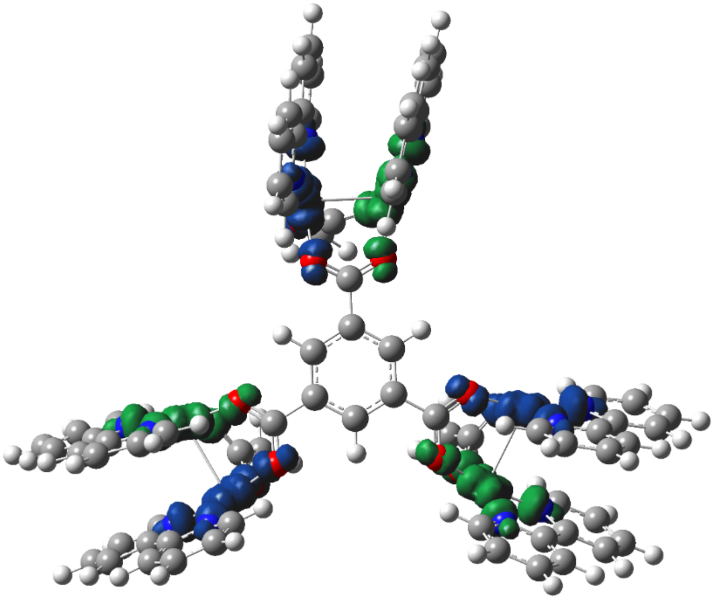

Figure S4. Spin density of in $[Cu_{24}(btc)_8(bipy)_{24}][ClO_4]_{24}$ after removal of methyoxy groups from optimized structure of $[Cu_{12}(btc)_4(OMe\text{-}bipy)_{12}][ClO_4]_{12}$

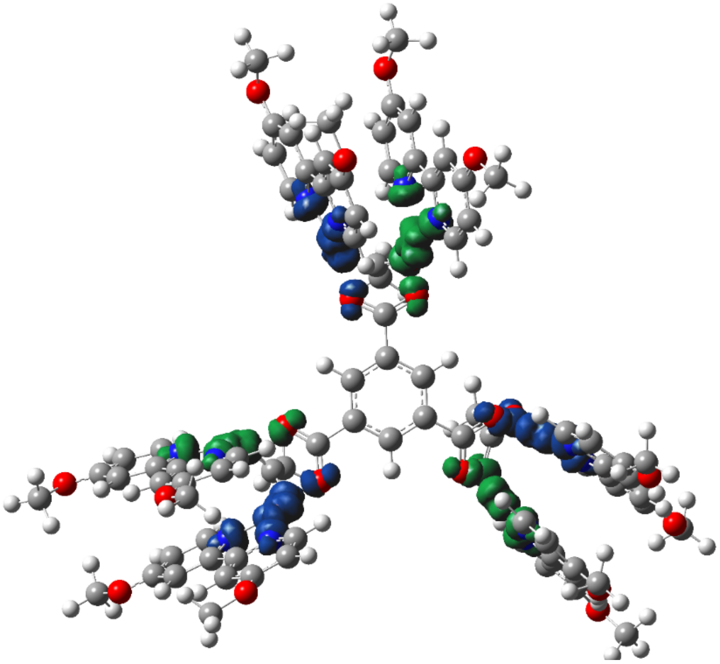

Figure S5. Spin density of $[Cu_{12}(btc)_4(OMe\text{-}bipy)_{12}][ClO_4]_{12}$

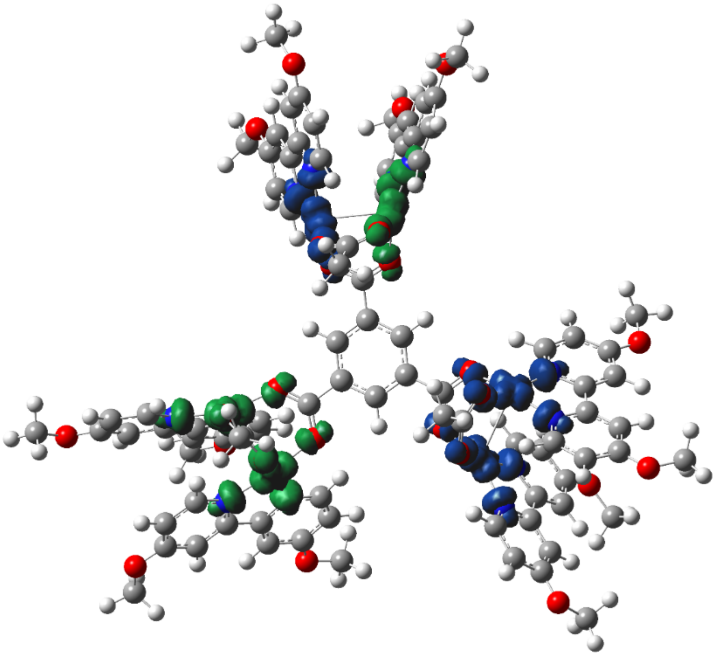

Figure S6. Spin density of $[Cu_{12}(btc)_4(OMe\text{-}bipy)_{12}][ClO_4]_{12}$with methoxy groups added to the optimized structure of $[Cu_{24}(btc)_8(bipy)_{24}][ClO_4]_{24}$.

Gas Adsorption Measurements

All gas adsorption isotherms were measured on a Micromeritics 3Flex gas adsorption analyzer. Hot sample tubes were affixed with seals and evacuated on a Smartvac system and weighed upon cooling. The sealed tubes were then brought into an N_2 glove box and filled with ~150 mg of sample. $Mo_{12}(btc)_4(DtolF)_{12}$ was activated under dynamic vacuum at room temperature. The copper samples were each activated at 100 °C under dynamic vacuum. Samples were considered activated when the static outgas rate was less than 2 μbar/min. Once fully activated, tubes were weighed to determine an accurate mass of each sample. Surface areas and pore volumes were measured via N_2 adsorption at 77 K or CO_2 adsorption at 195 K in a dry ice/isopropyl alcohol mixture.

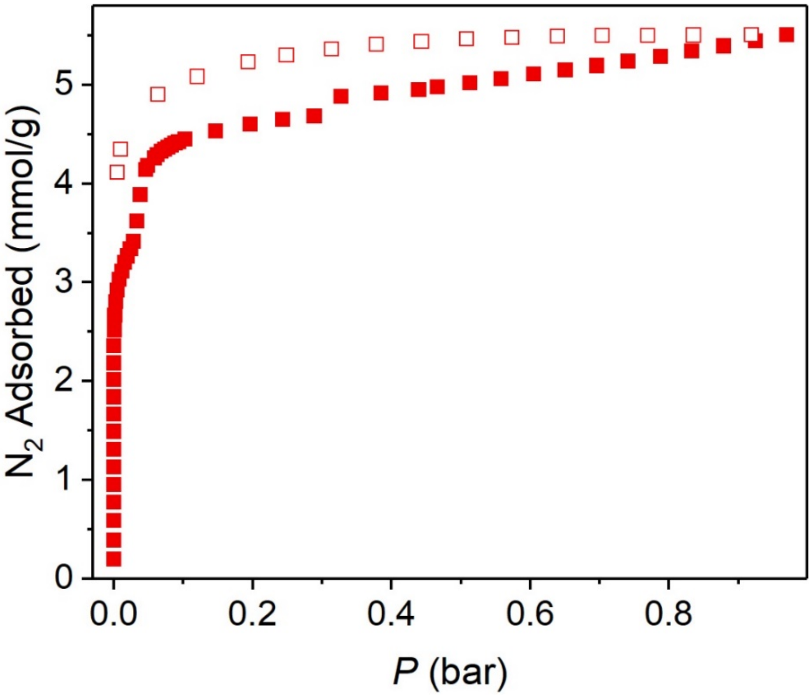

Figure S7. N_2 adsorption in $Mo_{12}(btc)_4(DtolF)_{12}$ at 77 K. The filled squares represent adsorption of N_2 while the open squares show desorption.

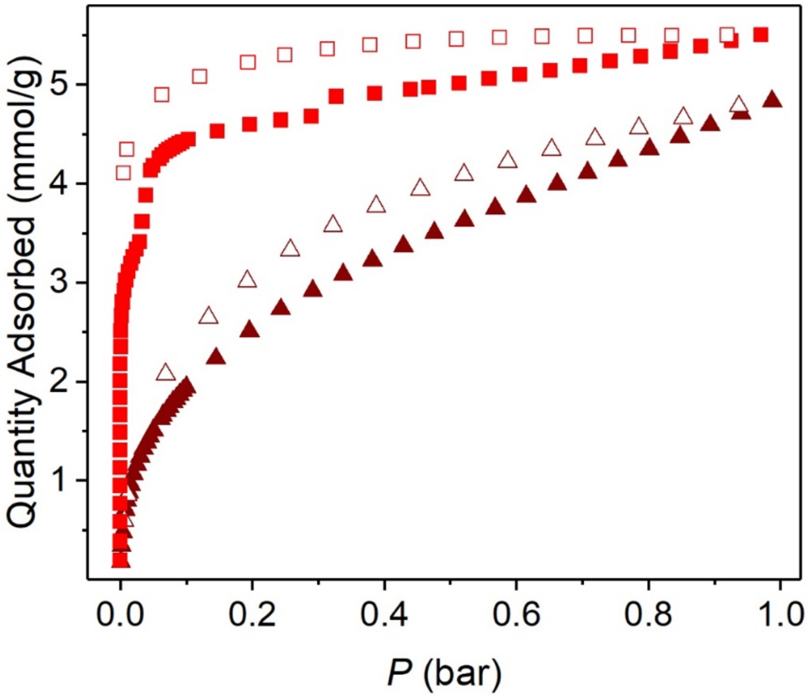

Figure S8. N_2 adsorption in $Mo_{12}(btc)_4(DtolF)_{12}$ at 77 K (red squares) and CO_2 adsorption at 195 K after rapidly removing solvent from a saturated CH_2Cl_2 solution (dark red triangles). The filled symbols represent adsorption while the open symbols are desorption.

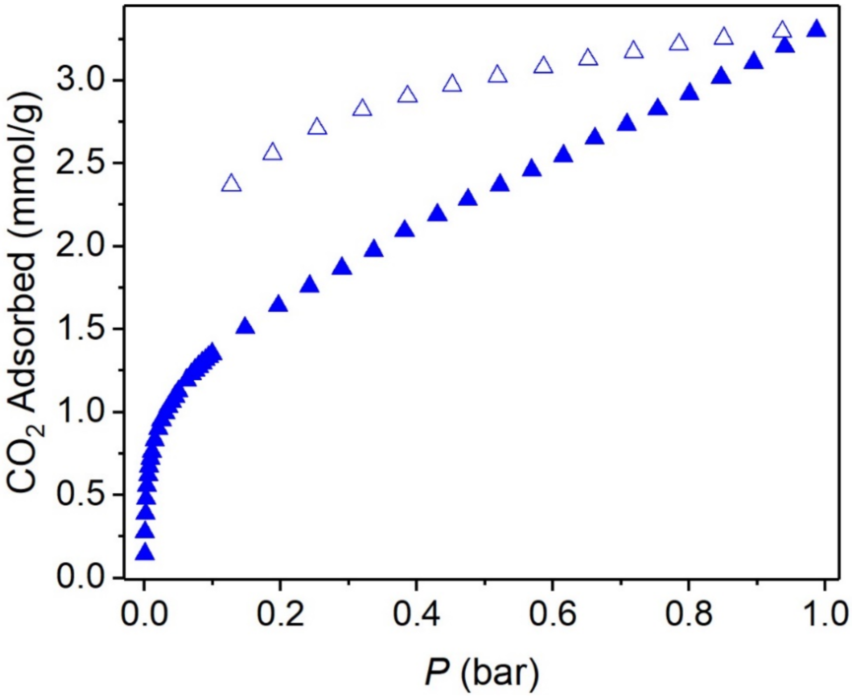

Figure S9. CO_2 adsorption in $[Cu_{24}(btc)_8(bipy)_{24}][ClO_4]_{24}$ at 195 K. The filled triangles represent adsorption of CO_2 while the open triangles show the desorption.

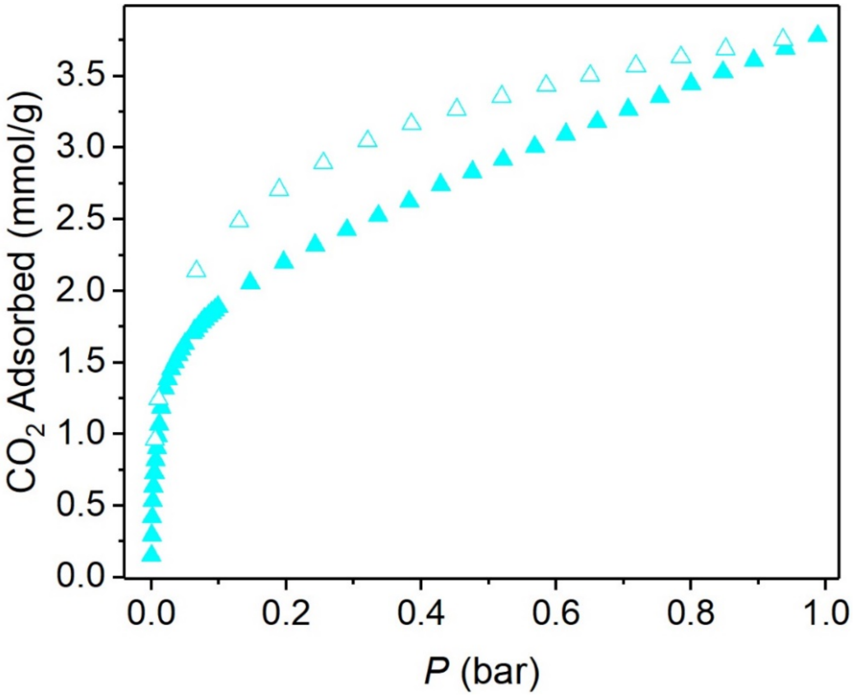

Figure S10. CO$_2$ adsorption in $[Cu_{12}(btc)_4(OMe\text{-}bipy)_{12}][ClO_4]_{12}$ at 195 K. The filled triangles represent adsorption of CO$_2$ while the open triangles show the desorption.

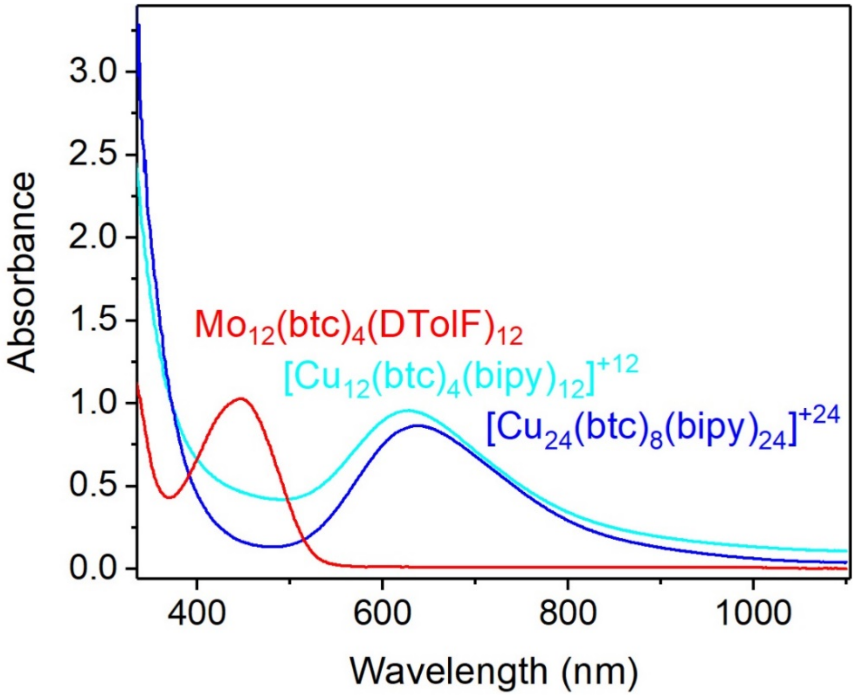

Figure S11. UV-Vis spectra for the indicated compounds. The Cu^{2+} cages were recorded in acetonitrile while the Mo^{2+} sample was in dichloromethane.

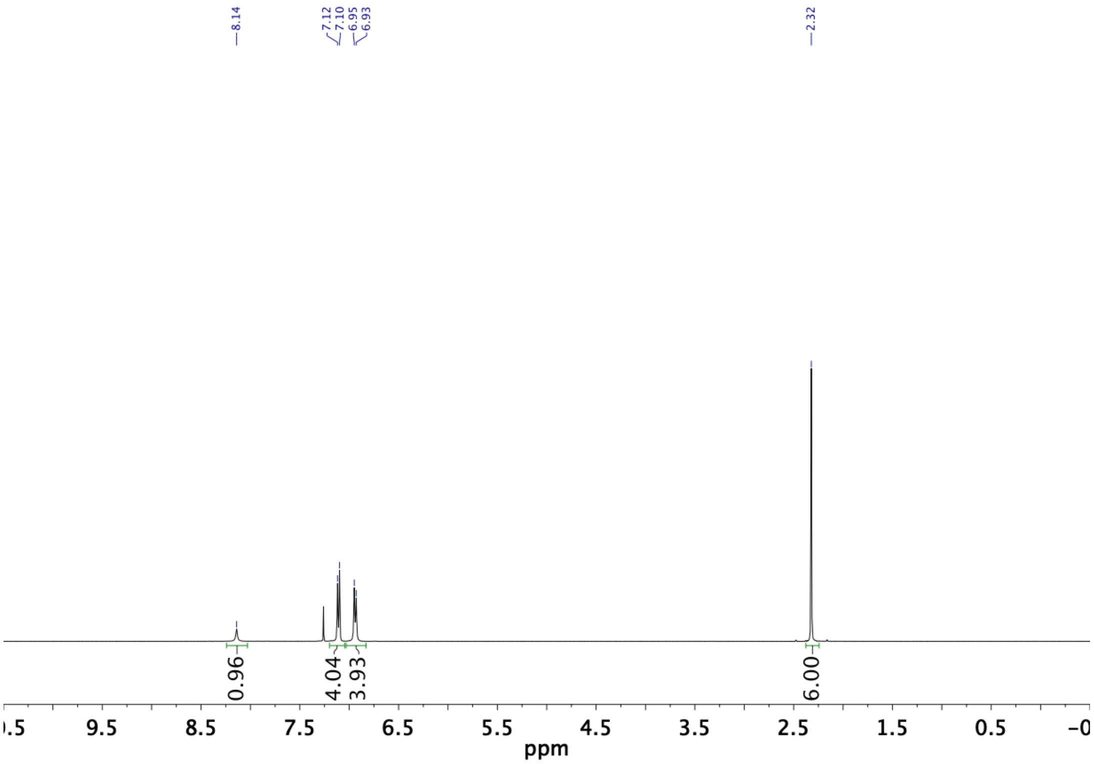

Figure S12. NMR spectra of HDTolF ligand.

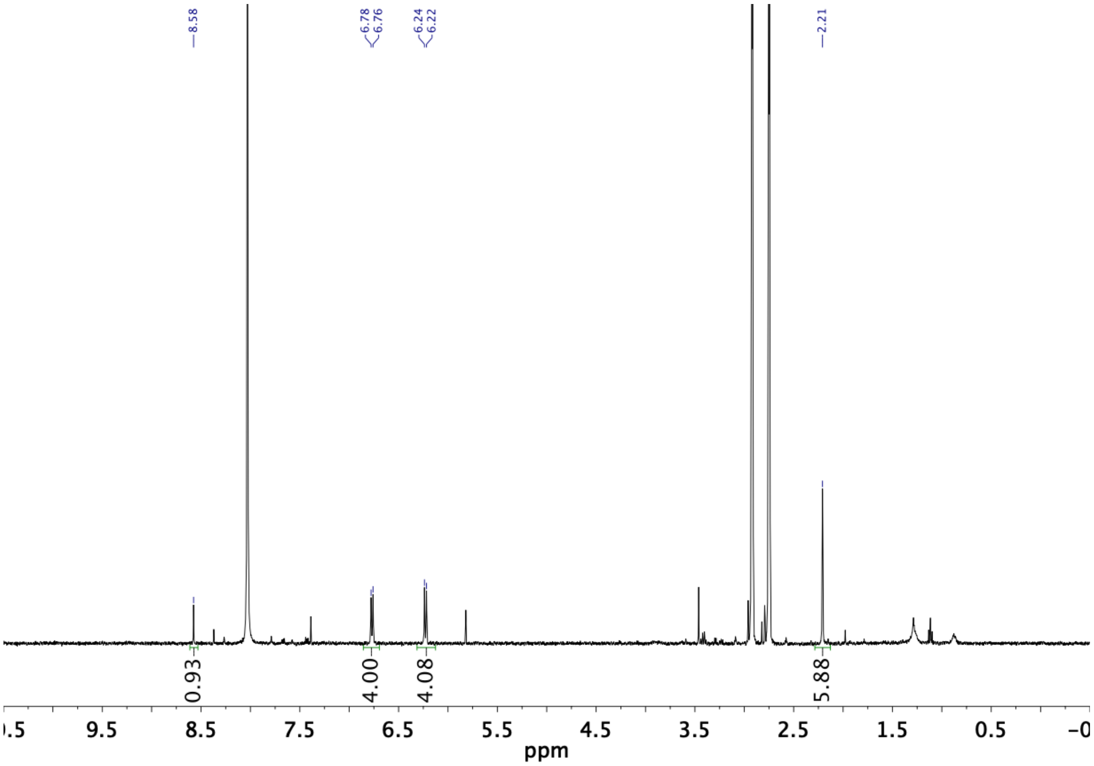

Figure S13. NMR spectra of $Mo_2(DTolF)_4$ paddlewheel.

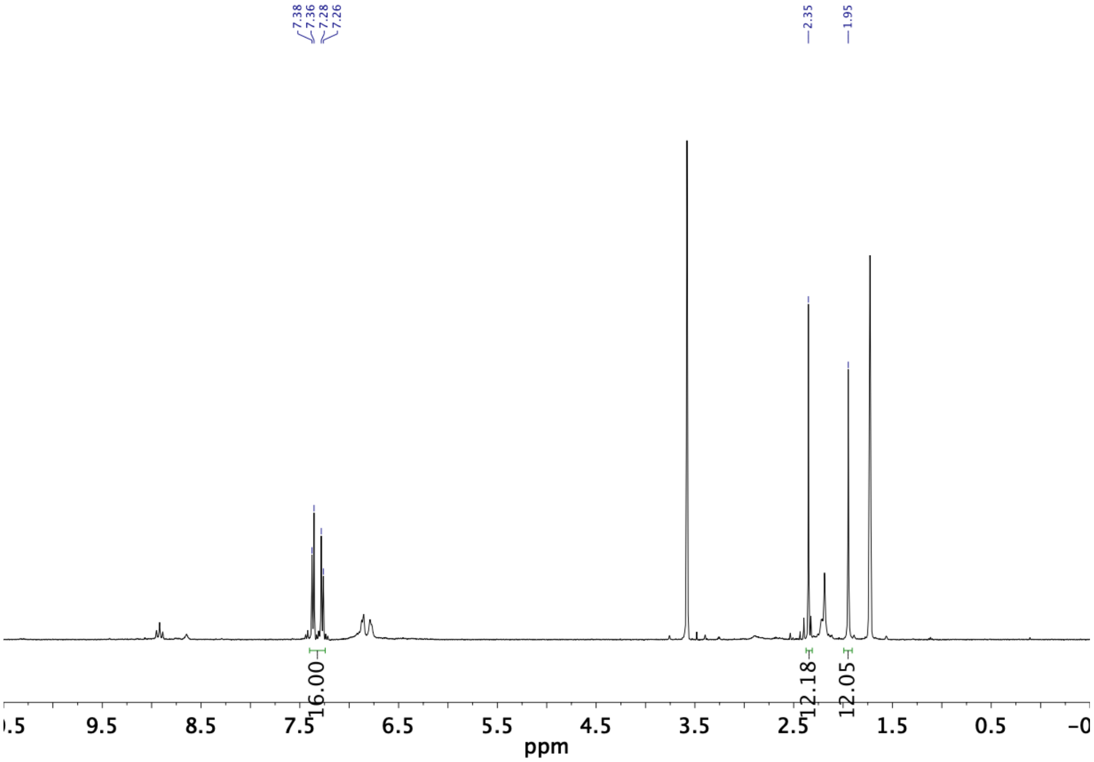

Figure S14. NMR spectra of *cis*-$[Mo_2(DTolF)_2(MeCN)_4][BF_4]_2$ complex.

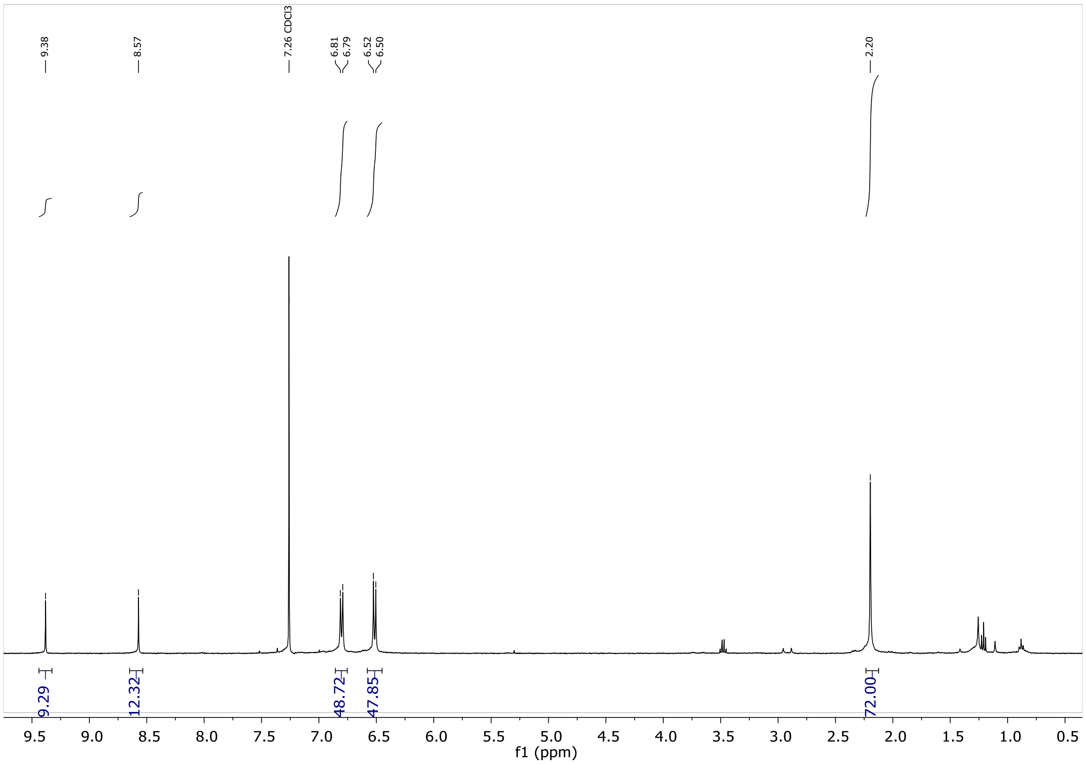

Figure S15. NMR spectra of $Mo_{12}(btc)_4(DtolF)_{12}$.

References

1. F. A. Cotton, X. Feng, M. Matusz, *Inorg. Chem*., 1989, **28**, 594-601.
2. M. Chrisholm, C. F. Albert, L. Daniels, J. Huffman, S. Iyer, A. Macintosh, C. Murillo, *Dalton Trans*., 1999, **9**, 1387-1392.
3. F. A. Cotton, L. M. Daniels, C. Lin, C. A. Murillo, *Chem. Comm*., 1999, **9**, 841-842.
4. W. R. McWhinnie, *J. Chem. Soc.*, 1964, 2959-2969.
5. S. P. Perlepes, J. C. Huffman, G. Christou, Polyhedra, 1992, **11**, 1471-1479.
6. Apex3; Bruker AXS Inc.: Madison, WI, 2015.
7. G. M. Sheldrick, *Acta. Cryst.,* 2015, **A71**, 3-8.
8. G. M. Sheldrick, *Acta. Cryst.*, 2015, **C71**, 3-8.
9. J. Park, Z. Perry, Y. -P. Chen, J. Bae, H. -C. Zhou, *ACS Appl. Mater. Interfaces*, 2017, **9**, 28064-28068
10. A. L. Spek, *Acta. Cryst.,* 2015, **C71**, 9-18.
11. Y. Zhao, D.G. Truhlar, *Theor. Chem. Acc.* 2008, **120**, 215.
12. P. C. Hariharan, J.A. Pople, *Theor. Chem. Acc.* 1973, **28**, 213.
13. M. J. Frisch, et.al. *Gaussian 09*; Gaussian, Inc.: Wallingford, CT, 2009.
14. K. Yamaguchi, Y. Takahara, T. Fueno, K. Nasu, *Jpn. J. Appl. Phys.* 1987, **26**, L1362.
15. K. Yamaguchi, F. Jensen, A. Dorigo, K. N. Houk, *Chem. Phys. Lett.* 1988, **149**, 537.
16. K. Yamaguchi, Y. Takahara, T. Fueno, K. N. Houk, *Theor. Chim. Acta* 1988, **73**, 337.